Proceedings of the International Gas Turbine Congress 2003 Tokyo
November 2-7, 2003

IGTC2003Tokyo TS-022

High Accuracy Multigrid Method of the Unsteady Convection Diffusion Equation and Calculations of Heat and Fluid Flow

Wenquan WU and Yongbin GE

College of Power Engineering
The University of Shanghai for Science and Technology
Shanghai 200093, China
Phone: 86-21-5553-0703, FAX: 86-21-6568-2258, E-mail: wqwu@sh163.net

ABSTRACT

A stable high order finite difference with a fully implicit time-marching scheme is proposed to solve the two-dimensional unsteady convection diffusion equation with variable coefficients. It is essentially compact and has the nice features of a compact scheme with regard to the treatment of boundary conditions. A time-dependent multigrid full approximation storage(FAS) scheme , which is suitable for both linear and nonlinear problem, is employed to accelerate convergence for the implicit scheme at each time step. Numerical simulations of the unsteady driven flow and natural convection in a square cavity are performed by the present method. The study demonstrates that the method developed here is very accurate, computationally efficient and is capable of performing accurate simulations of time-dependent, and possibly chaotic, flows in enclosures.

INTRODUCTION

Numerical solution of the convection diffusion equation plays a very important role in computational fluid dynamics and numerical heat transfer to simulate heat and fluid flow problems. Traditional finite difference discretization schemes such as the second-order central difference scheme and the first-order upwind scheme have the drawbacks of either lack of stability (central difference) or lack of accuracy (upwind). Recently, there has been growing interest in developing fourth-order finite difference schemes for the convection diffusion equation (and the Navier-Stokes equations) which give high accuracy approximations (Dennis,1989; Gupta , 1997; Zhang, 1997). Although considerable amount of work has done in the past, researchers are concerned more on steady problems(Dennis,1989; Gupta, 1997; Zhang, 1997) than unsteady ones which are studied by the characteristics difference method (Douglas ,1982) and the Group Explicit(GE) method(Evans, 1985). There is still a lack of a completely satisfactory computational (stability and accuracy) scheme that is suitable for all types of unsteady convection diffusion equations. Therefore, in this paper, for the two dimensional unsteady convection diffusion equation with variable coefficients

$$\phi_t + p(x,y,t)\phi_x + q(x,y,t)\phi_y - a(\phi_{xx} + \phi_{yy}) = f(x,y,t) \tag{1}$$

in which, the convection coefficients $p(x,y,t)$ and $q(x,y,t)$ are functions of the variables x, y and t and assumed to be sufficiently smooth. The diffusion coefficient a is constant.

Manuscript Received on March 28, 2003

Firstly, a fourth-order compact finite difference in the space directions and a second-order fully implicit time-marching scheme is presented; Then, a time-dependent multigrid FAS scheme is applied to accelerate convergence process when iterative methods are used to treat the implicit scheme at each time step; Finally, driven flow and natural convection in a square cavity as two test problems are simulated to examine accuracy and efficiency of our basic scheme's applications in the calculation of heat transfer and fluid flow.

HIGH ACCURACY DIFFERENCE SCHEME

Considering the classical BTCS scheme (Backward for Time and Center for Space), characteristics difference method (Douglas ,1982) and the GE method (Evans,1985),has only low order accuracy in space whereas improving the accuracy of schemes, especially that of convection terms, is very crucial and efficient for improving the stability, accuracy of schemes and decreasing the computational cost(by discretizing computational domain with comparably coarse grids). Therefore, in this paper, we firstly construct a high order compact full implicit difference scheme.

Assuming a uniform grid in both x- and y- directions, we number the grid points (x,y), (x+h,y), (x,y+h), (x-h,y), (x,y-h), (x+h,y+h), (x-h,y+h), (x-h,y-h) and (x+h,y-h) as 0, 1, 2, 3, 4, 5, 6, 7 and 8 respectively ,where h is the grid size. In writing the finite difference approximations, a single subscript j denotes the corresponding function value at the grid point numbered j. τ denotes time step size and $g_{ij} = g_i - g_j$, g can be ϕ , p , q etc.

Following the discretizing method by Ge (2003), a second-order backward Euler difference scheme for the time derivative term and making use of the fourth-order compact difference formula (Hirsh ,1975) for the second order space derivative terms while the first order derivative terms are discretized by center difference scheme but the third order derivative term is kept for modification. Finally we can get its fourth-order full implicit discretization scheme

$$\sum_{j=0}^{8} A_j^{n+1}\phi_j^{n+1} = \sum_{j=0}^{4} B_j^{n}\phi_j^{n} + \sum_{j=0}^{4} C_j^{n-1}\phi_j^{n-1} + F^{n+1} \tag{2}$$

in which

$$A_0^{n+1} = -[20 + h^2(p_0^2 + q_0^2)/a^2 - h(p_{13} + q_{24})/a + 6h^2/(a\tau)]$$

$$A_1^{n+1} = 4 - h(4p_0 + 3p_1 + p_{23} + p_4)/(4a) + h^2(4p_0^2 + p_0 p_{13} + q_0 p_{24})/(8a^2) + 3h^2(hp_0/a - 2)/(8a\tau)$$

$$A_2^{n+1} = 4 - h(4q_0 + q_1 + 3q_2 + q_{34})/(4a) + h^2(4q_0^2 + p_0 q_{13} + q_0 q_{24})/(8a^2) + 3h^2(hq_0/a - 2)/(8a\tau)$$

$$A_3^{n+1} = 4 + h(4p_0 + p_{41} + p_2 + 3p_3)/(4a) + h^2(4p_0^2 - p_0 p_{13} - q_0 p_{24})/(8a^2) - 3h^2(hp_0/a + 2)/(8a\tau)$$

$$A_4^{n+1} = 4 + h(4q_0 + q_{12} + q_3 + 3q_4)/(4a) + h^2(4q_0^2 - p_0 q_{13} - q_0 q_{24})/(8a^2) - 3h^2(hq_0/a + 2)/(8a\tau)$$

$$A_5^{n+1} = 1 - h(p_0 + q_0)/(2a) - h(q_{13} + p_{24})/(8a) + h^2 p_0 q_0/(4a^2)$$

$$A_6^{n+1} = 1 + h(p_0 - q_0)/(2a) + h(q_{13} + p_{24})/(8a) - h^2 p_0 q_0/(4a^2)$$

$$A_7^{n+1} = 1 + h(p_0 + q_0)/(2a) - h(q_{13} + p_{24})/(8a) + h^2 p_0 q_0/(4a^2)$$

$$A_8^{n+1} = 1 - h(p_0 - q_0)/(2a) + h(q_{13} + p_{24})/(8a) - h^2 p_0 q_0/(4a^2)$$

$$B_0^n = -8h^2/(a\tau)$$

$$B_1^n = h^2(hp_0/a - 2)/(2a\tau)$$

$$B_2^n = h^2(hq_0/a - 2)/(2a\tau)$$

$$B_3^n = -h^2(hp_0/a + 2)/(2a\tau)$$

$$B_4^n = -h^2(hq_0/a + 2)/(2a\tau)$$

$$C_0^{n-1} = 2h^2/(a\tau)$$

$$C_1^{n-1} = h^2(2 - hp_0/a)/(8a\tau)$$

$$C_2^{n-1} = h^2(2 - hq_0/a)/(8a\tau)$$

$$C_3^{n-1} = h^2(2 + hp_0/a)/(8a\tau)$$

$$C_4^{n-1} = h^2(2 + hq_0/a)/(8a\tau)$$

$$F^{n+1} = -h^2\left(\sum_{j=1}^{4} f_j^{n+1} + 8f_0^{n+1}\right)/(2a) + h^3(p_0 f_{13}^{n+1} + q_0 f_{24}^{n+1})/(4a^2)$$

in which, $n \geq 1$, and p, q in the coefficients A^{n+1}, B^n, and C^{n-1} correspond to the exact values on the $(n+1)$ th, n th and $(n-1)$ th temporal levels.

The Eq.(2) with the local truncation error $O(\tau^2 + h^4)$ is the high order implicit compact difference scheme for Eq.(1). We notice that it is a three-level scheme, which means that only we get the information on the first temporal level besides initial values computations can be continued. So, at the last step above, we just substitute the second Euler difference formula with classical backward difference, scheme for the first temporal level can be constructed.

MULTIGRID METHOD

To solve the large-scale discrete system that arises at each time step from the fully implicit time-marching scheme, conventional relaxation methods are much too inefficient. In order to obtain fast convergence, we use a multigrid method. The most important operator in the multigrid method is the relaxation operator(the smoother). Its role is not to remove the errors, but to damp the high frequency components of the errors on the current grid while leaving the low frequency components to be removed by the coarser grids. We employ the multigrid V-cycle scheme and point-SOR method as the smoothing operator. and the full-weighting restriction operator and the bi-linear interpolation operator For details, refer to (Brandt, 1977, Wesseling , 1992).

Considering the characteristics of the time-dependent equation and easy to be extended to nonlinear cases, we put forward a revised FAS scheme of multigrid which differs from the one used for the steady problems(Gupta,1997; Zhang, 1997) to obtain more accurate corrected results on the coarse grids. For simplicity of discussion, a two-level time-dependent FAS algorithm for a general equation of the form:

$$L_k^{n+1}\phi_k^{n+1} = L_k^n\phi_k^n + L_k^{n-1}\phi_k^{n-1} + f_k$$

may be described loosely as follows:

i) relax on $L_k^{n+1}\phi_k^{n+1} = L_k^n\phi_k^n + L_k^{n-1}\phi_k^{n-1} + f_k$

ii) solve $L_{k-1}^{n+1}\phi_{k-1}^{n+1} = L_{k-1}^{n+1}R_k^{k-1}\bar{\phi}_k^{n+1} - L_{k-1}^n R_k^{k-1}\bar{\phi}_k^n - L_{k-1}^{n-1}R_k^{k-1}\bar{\phi}_k^{n-1} + R_k^{k-1}(f_k + L_k^n\bar{\phi}_k^n + L_k^{n-1}\bar{\phi}_k^{n-1} - L_k^{n+1}\bar{\phi}_k^{n+1})$

iii) replace $\phi_k^{n+1} \leftarrow \phi_k^{n+1} + P_{k-1}^k(\phi_{k-1}^{n+1} - R_k^{k-1}\phi_k^{n+1})$

in which, L, R, P are difference operator, restriction operator and prolongation operator respectively and $\bar{\phi}$ is approximate value of ϕ. k represents spatial fine grid level and $k-1$ coarse grid level. $n+1, n, n-1$ represent temporal levels respectively.
In the process of the multigrid algorithm above, only dropping off all terms concerning with $n-1$ and let $n=0$, the multigrid algorithm on the first temporal level can be obtained.

NUMERICAL EXPERIMENTS

Driven cavity flow

As a model problem, we consider the incompressible viscous flow in a square cavity (0≤ x, y≤ 1). The flow is induced by sliding motion of the top wall from left to right and described by the

Navier-Stokes equations in vorticity-streamfunction formula:

$$\psi_{xx} + \psi_{yy} = -\xi \tag{3}$$

$$\xi_t + u\xi_x + v\xi_y = (\xi_{xx} + \xi_{yy})/\mathrm{Re} \tag{4}$$

The boundary conditions are those of no slip: on the stationary walls u=0 and v=0; on the sliding wall u=1 and v=0.

Heated cavity flow

Another model problem, we still consider a square cavity($0 \le$ x, y $\le$ 1) with differentially heated sidewalls and adiabatic top and bottom walls which is one of the classical problems in the field of heat transfer. For the case, the surface between the hot and cold walls are insulated. The governing equations are given in streamfunction-vorticity form as

$$\psi_{xx} + \psi_{yy} = -\xi \tag{5}$$

$$\xi_t + u\xi_x + v\xi_y = \mathrm{Pr}(\xi_{xx} + \xi_{yy}) + Ra\,\mathrm{Pr}\,T_x \tag{6}$$

$$T_t + uT_x + vT_y = T_{xx} + T_{yy} \tag{7}$$

with boundary conditions to be satisfied are $\psi = \psi_x = 0$, $T = 1$ on the hot wall; $\psi = \psi_x = 0$, $T = 0$ on the cold wall, and $\psi = \psi_y = 0$, $T_y = 0$ on the top and bottom walls.

In the two problems above, ψ, ξ and T represent the streamfunction, vorticity and temperature respectively. $u = \psi_y$ and $v = -\psi_x$ are velocity component at *x*- and *y*- direction respectively. Re , Pr and *Ra* are the non-dimensional Reynolds, Prandtl and Rayleigh numbers.

These two test problems, as the demonstration of accuracy and dependability of developed methods, have been studied by many researchers (Ghia, 1982; Paolucci, 1989; Bruneau 1990; Le Quéré 1991; Liu, 1993; Janssen ,1993; Nobile, 1996; Syrjälä , 1996). It has been shown that flows becomes unsteady for a value of Re larger than 5000 for driven flow (Liu H, 1993; Ge,2003) and *Ra* close to 2×10^8 when Pr equal 0.71 for natural convection in a square cavity (Paolucci,1989; Janssen, 1993).This was also confirmed very recently by Nobile, 1996).

Eq.(3) and (5) are Poisson type equations, we use the typical fourth order nine-point discretization (Tian , 1996):

$$4\sum_{j=1}^{4}\psi_j + \sum_{j=5}^{8}\psi_j - 20\psi_0 = -h^2\left(\sum_{j=1}^{4}\xi_j + 8\xi_0\right)/2$$

We notice that Eq.(4), (6) and (7) are all unsteady convection diffusion equations, consequently we can discretize them by using Eq.(2). Besides, u, v and T_x, the coefficients of first derivative terms ξ_x, ξ_y, T_x, T_y, are the unknown quantities, so they must be discretized by same order accuracy in order to obtain the full fourth order accuracy of the scheme, their discretized schemes are as follows:

$$u_2/6 + 4u_0/6 + u_4/6 = \psi_{24}/(2h) + O(h^4)$$

$$v_1/6 + 4v_0/6 + v_3/6 = -\psi_{13}/(2h) + O(h^4)$$

$$(T_x)_1/6 + 4(T_x)_0/6 + (T_x)_3/6 = T_{13}/(2h) + O(h^4)$$

The implementation of numerical boundary conditions has received considerable attention in the past. Usually vorticity conditions on the boundaries are employed and proved successful in practice. In this work, to agree with the high-order scheme, we make use of a fourth-order-accurate numerical boundary formulation proposed by Sptoz (1998)

$$h(6\xi_0 + 4\xi_1 - \xi_2)/21 + O(h^4) = (15\psi_0 - 16\psi_1 + \psi_2)/(14h) \pm V_w$$

and the boundary temperature $T_y = 0$ by Ge (2002)

$$T_0 = (18T_1 - 9T_2 + 2T_3)/11 + O(h^4)$$

where the subscript 0 denotes a value at a boundary grid point and the subscript j (j=1,2,3) denotes the value at the jth internal grid point along the inward normal at 0. Vw is the velocity on the wall. Vw=0 except on the moving wall where Vw =1 for the driven cavity.

All computations are done on Pentium III/1000 private computer using the Fortran 77 programming language in double precision. In the solution procedure, the result with lower Reynolds/ Rayleigh number is obtained at first, then the configurations with higher Reynolds/ Rayleigh number are solved by using the solution with lower Reynolds/ Rayleigh number as an initial value. The momentum and energy transport equations are solved by fully implicit time marching method.

In Table 1, there list all kinds of parameters used in the computation and time steps for obtaining convergent solutions for driven cavity flow. Computation results show that the accuracy of the method is independent of time increment for steady solution, so we can use big time increment. For instance, for Re=400, we can get convergent solution after eight time marching steps at τ =10 while 6000 time steps needed at τ =0.001 in reference (Liu, 1993). Table 2 reports the strength and location of the primary, secondary, and tertiary vortices for $\mathrm{Re} = 400$, 1000, 5000. For reference, the results obtained by Ghia (1982) and Nobile (1996) are listed.

Figures 1~4 show the velocity profiles for u along the vertical line and v along the horizontal line passing through the geometric center of the cavity for Re=400,1000 and 5000 respectively and streamline contours for Re=1000,5000, which agree well with the results of reference (Ghia U, 1982). However, when Re>5000, there is no steady laminar solution. Flow becomes unsteady and periodic. Figures 5~8 show the streamline contours for Re=7500 and 10000 at t=60 and the time histories of their velocities at point (0.5,0.5) respectively. Through observation, we can discover that the time period is about 6.58 for Re=7500 and 6.75 for Re=10000 while 6.56 and 6.36 respectively in the reference (Liu, 1993).

For the heated cavity flow, we use V(2,2) multigrid cycle. Numerical results when Pr=0.71 and *Ra* from 10^3 to 10^7 are considered. Table 3 compare the present results for $Ra = 10^3$, 10^4, 10^5, 10^6 and 10^7 with the benchmark solutions in de Vahl Davis (1983), the compact difference solutions in Dennis and Hudson(1989), the results from Le Quéré(1991), who solved the problems using a pseudo-spectral Chebyshev algorithm, and the finite element solutions in Syrjälä(1996). This table show the excellent agreement of the present results with those of the benchmark solution and stable fourth-order method for all the values of *Ra* from 10^3 to 10^6, with those of the compact difference method up

to 10^5, with those of Le Qu ér é(1991) for $Ra = 10^6$ and 10^7, and with those of finite element method for $Ra = 10^5$ and 10^6. We use 32×32 grids for $Ra = 10^3$, 64×64 grids for $Ra = 10^4$ and 10^5, 128×128 grids for $Ra = 10^6$ and 10^7. For all multigrid cycles, the number on the coarsest grids is 4×4. The time steps are selected as $\tau = 20$ for $Ra = 10^3$, $\tau = 2.5$ for $Ra = 10^4$, $\tau = 0.25$ for $Ra = 10^5$, $\tau = 0.005$ for $Ra = 10^6$ and $\tau = 0.00025$ for $Ra = 10^7$.

Figures9~12 contain level curves for Streamline contour and isothermal lines plots. An analysis of pictures shows that the flux is symmetric with respect to the center for every Ra. At $Ra = 10^4$ the main feature of the flow is a central elliptic vortex, and the heat transfer is mainly due to conduction (vertical isotherms). For $Ra = 10^5$, the vortex breaks into two vortices moving toward the vertical walls for higher values of Ra, a third, weaker vortex is observed. Increasing Ra causes a changer of heat transfer mechanism. In fact, convection tends to become dominant: The isotherms are vertical everywhere, being horizontal only in the neighborhood of vertical walls (very thin thermal boundary layer).

CONCLUDING REMARKS

In this work, a high accuracy muligrid solver based on the fourth-order compact implicit difference scheme and time -dependent FAS scheme for general unsteady convection-diffusion equation is constructed. The time-dependent heat and fluid flows in a two-dimensional square cavity have been studied numerically.

Its accuracy has been verified for the well-known driven cavity flow problem, where the results on coarser meshes agree well with previous numerical results on finer grids for $\mathrm{Re} \le 5000$. In addition, fine-grid results have illustrated the unsteady flow dynamics when Re=7500 and Re=10000, which is in good agreement with results in the literatures.

Fully implicit time-marching scheme overcomes the inefficiency of explicit scheme only when time increment is small enough to keep computation convergence, e.g. τ = 0.001~0.002 (Liu, 1993). Computation results show that the accuracy of the method are independent of time increment for $\mathrm{Re} \le 5000$, so we can use big time increment to shorten the process of convergence to steady solution. Besides, for unsteady and periodic solution when Re=7500 and Re=10000, we can still use considerably big time increment e.g. τ =0.1.

The suitability of the proposed method to compute buoyant flows has been demonstrated by the calculation of the flow in a side-heated cavity, for fluids with Pr values of 0.71, Ra from 1×10^3 to 1×10^7. Close agreement is found for all the character -ristic quantities with the data reported in literatures.

Furthermore, it seems to promise to be a very efficient and accurate approach for more practical problems including three dimensions and complicated flows.

References

Brandt A, 1977, "A. Multi-Level Adaptive Solution to Boundary-Value Problems," *Mathematics of Computation*, Vol. 31, pp. 333-390.

Bruneau C H and Jouron C, 1990, "An Efficient Scheme for Solving Steady Incompressible Navier-Stokes Equations," *Journal of Computational Physics*, Vol. 89, pp. 389-413.

De Vahl Davis G, 1983, Natural Convection in a Square Cavity: a Bench Mark Numerical Solution. *International Journal for Numerical Methods in Fluids*, Vol. 3 , pp.2 4 9~264.

Dennis S C R and Hudson J D, 1989, "Compact h^4 Finite-Difference Approximations to Operators of Navier -Stokes Type," *Journal of Computational Physics*, Vol. 85, pp. 390-416.

Douglas J and Russel T F, 1982, "Numerical Method for Convection-Dominated Diffusion Problems Based on Combining the Method of Characteristics with Finite Element or Finite Difference Procedures," *SIAM Journal of Numerical Analysis*, Vol. 19, pp. 871-885.

Evans D J and Abdullah A R, 1985, "A New Explicit Method for the Diffusion-convection Equation," *Computers & Mathematics with Application*, Vol. 11, pp.145-154.

Ge Y B et al, 2002, "High Accuracy Multigrid Method for Two-Dimensional Diffusion Equation," *Journal of Engineering Thermophysics (in Chinese)*, Vol. 23, pp. 121-124.

Ge Y B et al, 2003, "Simulation of Time-Dependent Viscous Flows in an Cavity with High Accuracy Multigrid Method," *Journal of Engineering Thermophysics (in Chinese)*, Vol. 24, pp. 216 -219.

Ghia U et al, 1982, "High-Re Solutions for Incompressible Flow Using the Navier-Stokes Equations and a Multigrid Method," *Journal of Computational Physics*, Vol.48, pp.387-411.

Gupta M M et al, 1997, "A Compact Multigrid Solver for Convection-Diffusion Equations," *Journal of Computational Physics*, Vol.132, pp.123-129.

Hirsh R S, 1975, "Higher Order Accurate Difference Solutions of Fluid Mechanics Problem by a Compact Differencing Technique," *Journal of Computational Physics*, Vol.19, pp. 90 -109.

Janssen R J and Henkes R A, 1993, "Accuracy of Finite -Volume Discretizations for the Bifurcating Natural-Convection Flow in a Square Cavity," *Numerical Heat Transfer ,Part B*, Vol. 24, pp. 191-207.

Le Quéré , 1991, " Accurate Solution to the Square Thermally Driven Cavity at High Rayleigh Number". *Computers & Fluids*, Vol 20, 29~41

Liu H et al, 1993, "Upwind Compact Method and Direct Numerical Simulation of Driven Flow in a Square Cavity," *Science In China (Series A)* , Vol. 36, pp. 1347-1357.

Nobile E, 1996, "Simulation of the Time-Dependent Flow in Cavities with the Additive-Correction Multigrid Method. Part II: Applications," *Numerical Heat Transfer, Part B*, Vol.30, pp. 351-370.

Paolucci S and Chenoweth D R, 1989, "Transition to Chaos in Differentially Heated Vertical Cavity," *Journal of Fluid Mechanics*, Vol.210, pp.379-410.

Spotz W F, 1998, "Accuracy and Performance of Numerical Wall Boundary Condition for Steady 2D Incompressible Streamfunction-Vorticity," *International Journal for Numerical Methods in Fluids*, Vol.128, pp.737-757.

Syrjälä S, 1996, "Higher Order Penalty-Galerkin Finite Element Approach to Laminar Natural Convection in a Square Cavity." *Numerical Heat Transfer, Part A*, Vol. 29, pp.197~210

Tian Z F, 1996, "Compact High-Order Difference Methods for Solving the Poisson Equation," *Journal of Northwest University (in Chinese)*, Vol.26, pp.109-114.

Wesseling P W, 1992, "An Introduction to Multigrid Methods," Wiley & Sons, Chichester.

Zhang J, 1997, "Accelerated Multigrid High Accuracy Solution of the Convection-Diffusion Equation with High Reynolds Number," *Numerical Methods for Partial Differential Equations*, Vol. 13, pp.77-92.

APPENDIX: HIGH ACCURACY DIFFERENCE SCHEME FOR 3D CONVECTION DIFFUSION EQUATION

For the three-dimensional (3D) unsteady convection diffusion equation with variable coefficients

$$\phi_t + p(x,y,z,t)\phi_x + q(x,y,z,t)\phi_y + r(x,y,z,t)\phi_z - a(\phi_{xx} + \phi_{yy} + \phi_{zz}) = f(x,y,z,t)$$

in which, the convection coefficients p, q, r are functions of the

variables x, y, z and t and assumed to be sufficiently smooth. The diffusion coefficient a is constant. The fourth-order full implicit discretization scheme is

$$\sum_{j=0}^{18} A_j^{n+1}\phi_j^{n+1} = \sum_{j=0}^{6} B_j^n \phi_j^n + \sum_{j=0}^{6} C_j^{n-1}\phi_j^{n-1} + F^{n+1}$$

in which

$$A_0^{n+1} = -[24 + h^2(p_0^2 + q_0^2 + r_0^2)/a^2 - h(p_{1,3} + q_{2,4} + r_{5,6})/a + 9h^2/(2a\tau)]$$

$$A_1^{n+1} = 2 + h(2p_0 - 3p_1 - p_2 + p_{3,4} - p_5 - p_6)/(4a) + h^2(4p_0^2 + p_0 p_{1,3} + q_0 p_{2,4} + r_0 p_{5,6})/(8a^2) + 3h^2(hp_0/a - 2)/(8a\tau)$$

$$A_2^{n+1} = 2 + h(2q_0 - q_1 - 3q_2 - q_3 + q_{4,5} - q_6)/(4a) + h^2(4q_0^2 + p_0 q_{1,3} + q_0 q_{2,4} + r_0 q_{5,6})/(8a^2) + 3h^2(hq_0/a - 2)/(8a\tau)$$

$$A_3^{n+1} = 2 - h(2p_0 + p_{1,2} - 3p_3 - p_4 - p_5 - p_6)/(4a) + h^2(4p_0^2 - p_0 p_{1,3} - q_0 p_{2,4} - r_0 p_{5,6})/(8a^2) - 3h^2(hp_0/a + 2)/(8a\tau)$$

$$A_4^{n+1} = 2 - h(2q_0 - q_1 + q_{2,3} - 3q_4 - q_5 - q_6)/(4a) + h^2(4q_0^2 - p_0 q_{1,3} - q_0 q_{2,4} - r_0 q_{5,6})/(8a^2) - 3h^2(hq_0/a + 2)/(8a\tau)$$

$$A_5^{n+1} = 2 + h(2r_0 - r_1 - r_2 - r_3 - r_4 - 3r_5 + r_6)/(4a) + h^2(4r_0^2 + p_0 r_{1,3} + q_0 r_{2,4} + r_0 r_{5,6})/(8a^2) + 3h^2(hr_0/a - 2)/(8a\tau)$$

$$A_6^{n+1} = 2 - h(2r_0 - r_1 - r_2 - r_3 - r_4 + r_5 - 3r_6)/(4a) + h^2(4r_0^2 - p_0 r_{1,3} - q_0 r_{2,4} - r_0 r_{5,6})/(8a^2) - 3h^2(hr_0/a + 2)/(8a\tau)$$

$$A_7^{n+1} = 1 - h(p_0 + q_0)/(2a) - h(q_{1,3} + p_{2,4})/(8a) + h^2 p_0 q_0/(4a^2)$$

$$A_8^{n+1} = 1 + h(p_0 - q_0)/(2a) + h(q_{1,3} + p_{2,4})/(8a) - h^2 p_0 q_0/(4a^2)$$

$$A_9^{n+1} = 1 + h(p_0 + q_0)/(2a) - h(q_{1,3} + p_{2,4})/(8a) + h^2 p_0 q_0/(4a^2)$$

$$A_{10}^{n+1} = 1 - h(p_0 - q_0)/(2a) + h(q_{1,3} + p_{2,4})/(8a) - h^2 p_0 q_0/(4a^2)$$

$$A_{11}^{n+1} = 1 - h(p_0 + r_0)/(2a) - h(p_{5,6} + r_{1,3})/(8a) + h^2 p_0 r_0/(4a^2)$$

$$A_{12}^{n+1} = 1 - h(q_0 + r_0)/(2a) - h(q_{5,6} + r_{2,4})/(8a) + h^2 q_0 r_0/(4a^2)$$

$$A_{13}^{n+1} = 1 + h(p_0 - r_0)/(2a) + h(p_{5,6} + r_{1,3})/(8a) - h^2 p_0 r_0/(4a^2)$$

$$A_{14}^{n+1} = 1 + h(q_0 - r_0)/(2a) + h(q_{5,6} + r_{2,4})/(8a) - h^2 q_0 r_0/(4a^2)$$

$$A_{15}^{n+1} = 1 - h(p_0 - r_0)/(2a) + h(p_{5,6} + r_{1,3})/(8a) - h^2 p_0 r_0/(4a^2)$$

$$A_{16}^{n+1} = 1 - h(q_0 - r_0)/(2a) + h(q_{5,6} + r_{2,4})/(8a) - h^2 q_0 r_0/(4a^2)$$

$$A_{17}^{n+1} = 1 + h(p_0 + r_0)/(2a) - h(p_{5,6} + r_{1,3})/(8a) + h^2 p_0 r_0/(4a^2)$$

$$A_{18}^{n+1} = 1 + h(q_0 + r_0)/(2a) - h(q_{5,6} + r_{2,4})/(8a) + h^2 q_0 r_0/(4a^2)$$

$$B_0^n = -6h^2/(a\tau)$$

$$B_1^n = h^2(hp_0/a - 2)/(2a\tau)$$

$$B_2^n = h^2(hq_0/a - 2)/(2a\tau)$$

$$B_3^n = -h^2(hp_0/a + 2)/(2a\tau)$$

$$B_4^n = -h^2(hq_0/a + 2)/(2a\tau)$$

$$B_5^n = h^2(hr_0/a - 2)/(2a\tau)$$

$$B_6^n = -h^2(hr_0/a + 2)/(2a\tau)$$

$$C_0^{n-1} = 3h^2/(2a\tau)$$

$$C_1^{n-1} = h^2(2 - hp_0/a)/(8a\tau)$$

$$C_2^{n-1} = h^2(2 - hq_0/a)/(8a\tau) \qquad C_6^{n-1} = h^2(2 + hr_0/a)/(8a\tau)$$

$$C_3^{n-1} = h^2(2 + hp_0/a)/(8a\tau)$$

$$F^{n+1} = -h^2(\sum_{j=1}^{6} f_j^{n+1} + 6f_0^{n+1})/(2a)$$

$$C_4^{n-1} = h^2(2 + hq_0/a)/(8a\tau) \qquad + h^3(p_0^{n+1} f_{1,3}^{n+1} + q_0^{n+1} f_{2,4}^{n+1} + r_0^{n+1} f_{5,6}^{n+1})/(4a^2)$$

$$C_5^{n-1} = h^2(2 - hr_0/a)/(8a\tau)$$

Table 1 Parameters used in the computation and status of convergence

Re	Grid point	Grid levels	V-cycle	Time-increment	Time steps needed
400	64×64	five	V(1,1)	10	8
1000	64×64	five	V(1,1)	10	8
3200	128×128	four	V(1,1)	1	37
5000	128×128	four	V(1,1)	0.5	107
7500	256×256	three	V(2,2)	0.1	periodic solution
10000	256×256	three	V(2,2)	0.1	periodic solution

Table 2 Comparison of extreme value of streamfunction

	Primary vortex ψ (location)	Secondary vortex, bottom Right, ψ (location)	Secondary vortex, bottom left, ψ (location)
	Re=400		
Ghia et al (256×256)	-0.1139 (0.5547,0.6055)	6.42E-4 (0.8906,0.1250)	1.42E-5 (0.0508,0.0469)
Nibile (96×96)	-0.1131 (0.5521,0.6042)	6.59E-4 (0.8854,0.1250)	1.53E-5 (0.0521,0.0521)
Present (64×64)	-0.1135 (0.5469,0.6094)	6.59E-4 (0.8906,0.1250)	1.37E-5 (0.0469,0.0469)
	Re=1000		
Ghia et al (128×128)	-0.1179 (0.5313,0.5625)	1.75E-3 (0.8594,0.1094)	2.31E-4 (0.0859,0.0781)
Nibile (128×128)	-0.1175 (0.5313,0.5625)	1.77E-3 (0.8594,0.1094)	2.32E-4 (0.0859,0.0781)
Present (64×64)	-0.1166 (0.5313,0.5625)	1.87E-3 (0.8594,0.1094)	1.97E-4 (0.0781,0.0781)
	Re=5000		
Ghia et al (256×256)	-0.1189 (0.5117,0.5352)	3.08E-3 (0.8086,0.0742)	1.36E-3 (0.0703,0.1367)
Present (128×128)	-0.1184 (0.5078,0.5467)	3.42E-3 (0.7969,0.0781)	1.01E-3 (0.0781,0.1250)

Table3 Comparison of results with literatures when $\Pr = 0.71$ for different Ra

	$\lvert\psi_{mid}\rvert$	$\lvert\psi\rvert_{\max}$	$u_{\max}$	$v_{\max}$	Nu_0	$Nu_{\max}$	$Nu_{\min}$
			$Ra = 10^3$				
present	1.1742	1.1742	3.6481	3.6901	1.1181	1.5078	0.6905
Dennis et al	1.1747	n.a	3.6497	3.6977	1.1176	1.5058	0.6913
De Vahl Davis	1.174	n.a	3.649	3.697	1.117	1.505	0.692
			$Ra = 10^4$				
present	5.0719	5.0719	16.1692	19.5929	2.2450	3.5327	0.5844
Dennis et al	5.0735	n.a	16.1829	19.6293	2.2396	3.5193	0.5851
De Vahl Davis	5.071	n.a	16.178	19.617	2.238	3.528	0.586
			$Ra = 10^5$				
present	9.1104	9.6056	34.6163	68.5578	4.5097	7.7196	0.7203
Dennis et al	9.1126	n.a	34.716	68.637	4.4959	7.6830	0.7279
De Vahl Davis	9.111	9.612	34.73	68.59	4.509	7.717	0.729
			$Ra = 10^6$				
present	16.4107	16.8412	64.7611	220.246	8.7719	17.5445	0.9589
De Vahl Davis	16.320	16.750	64.63	219.36	8.817	17.925	0.989
Le Qu ér é	16.3864	16.8111	64.8344	220.559	8.8252	17.5360	0.9795
Syrjälä	16.3863	n.a	64.833	220.56	8.8251	n.a	n.a
			$Ra = 10^7$				
present	29.4326	30.2061	148.8537	699.091	16.4021	39.5376	1.2987
Le Qu ér é	29.361	30.165	148.59	699.17	16.523	39.39	1.366
Syrjälä	29.3616	n.a	148.593	699.506	16.5299	n.a	n.a

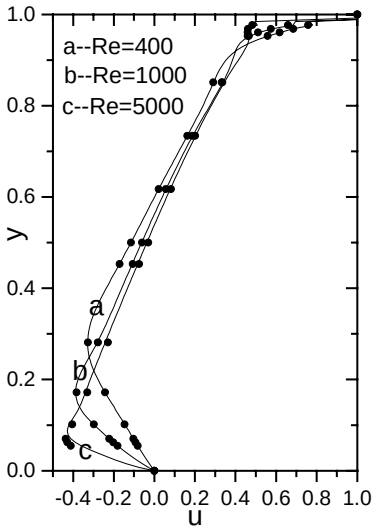

Fig1 Profiles of *u*-velocity along vertical lines through geometric center

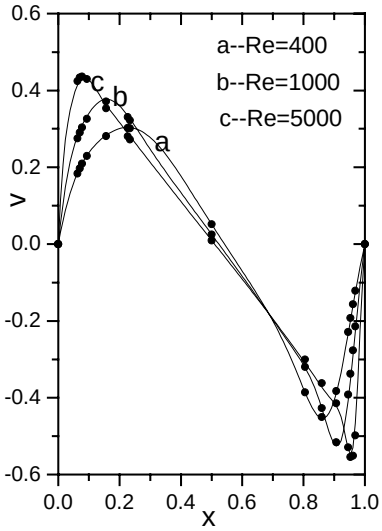

Fig2 Profiles of *v*-velocity along horizontal lines through geometric center

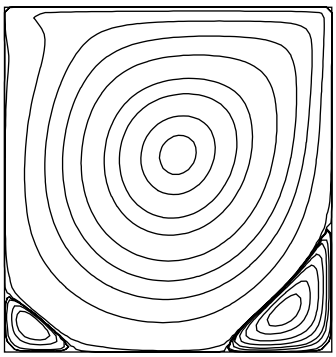

Fig 3 Streamfunction contours for Re=1000

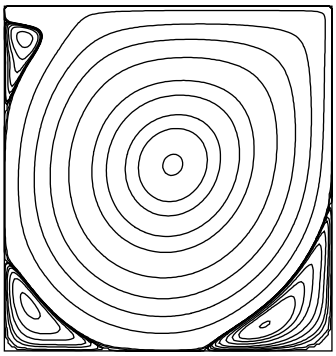

Fig4 Streamfunction contours for Re=5000

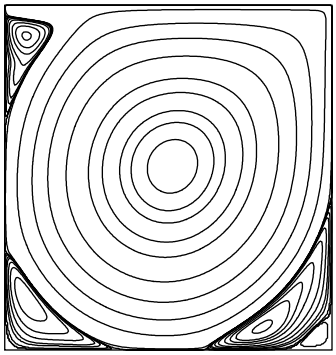

Fig. 5 Streamfunction contours for Re=7500

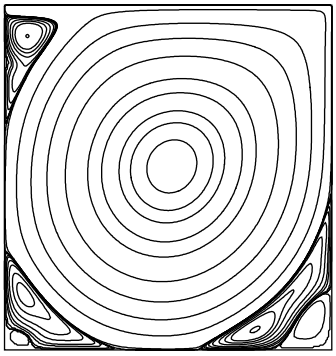

Fig. 6 Streamfunction contours for Re=10000

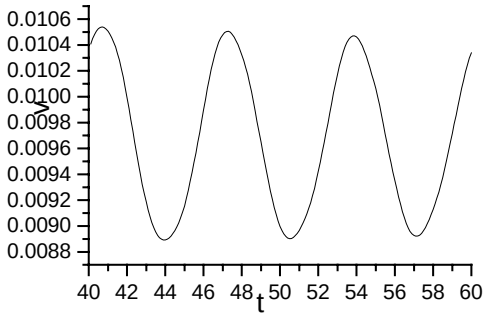

Fig 7 Time history of *v*-velocity for Re=7500

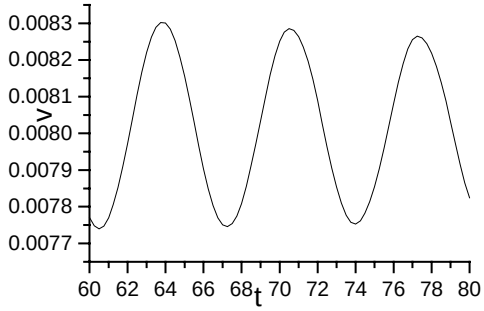

Fig 8 Time history of *v*-velocity for Re=10000

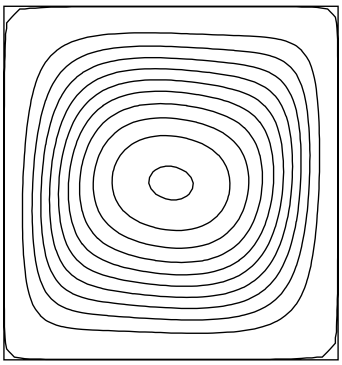

Fig.9a Streamlines for $Ra=10^4$

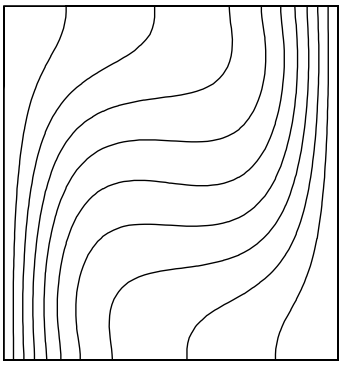

Fig.9b Isothermal lines for $Ra=10^4$

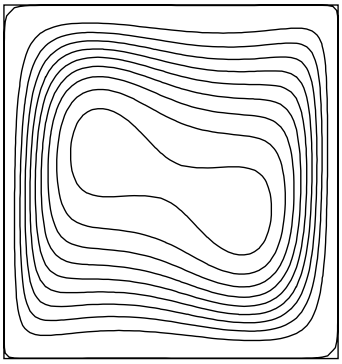

Fig.10a Streamlines for $Ra=10^5$

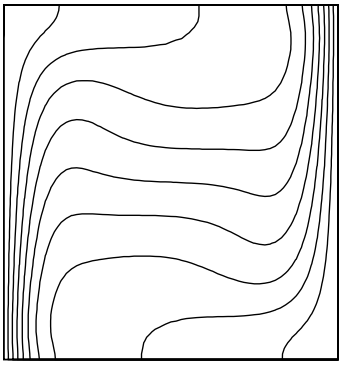

Fig.10b Isothermal lines for $Ra=10^5$

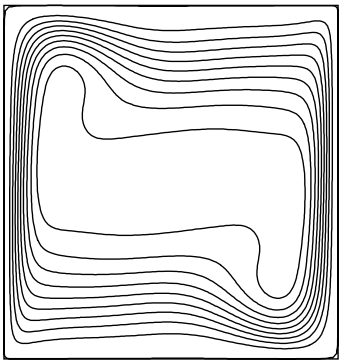

Fig.11a Streamlines for $Ra=10^6$

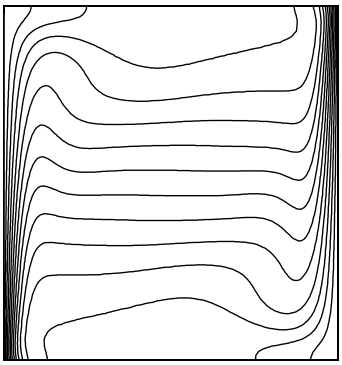

Fig.11b Isothermal lines for $Ra=10^6$

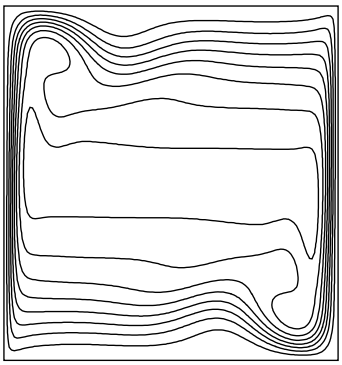

Fig.12a Streamlines for $Ra=10^7$

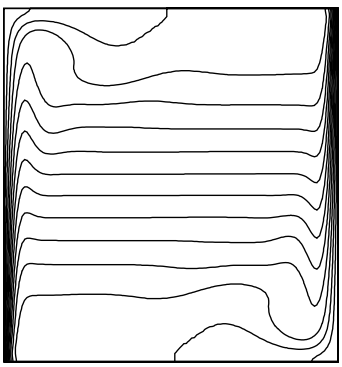

Fig.12b Isothermal lines for $Ra=10^7$